

# Optical Properties and Electronic Band Structure of Topological Insulators on $A_2^5B_3^6$ compound based

Husnu Koc  
Department of Physics, Siirt State University  
Siirt, Turkey  
husnu\_01\_12@hotmail.com

Amirullah M.Mamedov, Ekmel Ozbay  
Bilkent University, 06800 Bilkent  
Ankara, Turkey  
mamedov@bilkent.edu.tr, ozbay@bilkent.edu.tr

**Abstract**—We have performed a first principles study of structural, electronic, and optical properties of rhombohedral  $Sb_2Te_3$  and  $Bi_2Te_3$  compounds using the density functional theory within the local density approximation. The lattice parameters, bulk modulus, and its pressure derivatives of these compounds have been obtained. The linear photon-energy dependent dielectric functions and some optical properties such as the energy-loss function, the effective number of valance electrons and the effective optical dielectric constant are calculated and presented in the study

**Keywords**—*ab initio calculation; electronic structure; optical properties*

## I. INTRODUCTION

$Sb_2Te_3$  and  $Bi_2Te_3$ , the members of compounds with the general formula  $A_2^V B_3^{VI}$  ( $A=Bi, Sb$  and  $B=S, Se, Te$ ), are narrow-bandgap semiconductors with rhombohedral layered crystal structure.  $Sb_2T_3$  and  $Bi_2Te_3$  are well-known topological insulators [1-7], extraordinary thermoelectric materials at ambient temperature [8] and the possible topological superconductors [9] with surface states consisting of a single Dirac cone at the  $\Gamma$ . All of these have made  $A_2B_3$  compounds as the subject of intensive investigation both in fundamental and applied research. These compounds possess the rhombohedral crystal structure with five atoms per unit cell belonging to the space group  $D_{3d}^5(R\bar{3}m)$ .  $Sb_2T_3$  and  $Bi_2Te_3$  can be used for many different applications such as power generation and cooling devices [10]. Thermoelectric power generators and cooler have many advantages over conventional refrigerators and power generators such as long life, no moving parts, no green house gases, no noise, low maintenance and high reliability [11-13].

In the past, some detailed works [6, 7, 14, 15] have been carried out on the structural and electronic properties of these compounds. Zhang et al [6] study in detail the topological nature and the surface states of this family of compounds using the fully self-consistent *ab initio* calculations in the framework of density functional theory. Zhang et al [7] focus on layered, stoichiometric crystals  $Sb_2T_3$ ,  $Sb_2Se_3$ ,  $Bi_2Te_3$  and  $Bi_2S_3$  using *ab initio* calculations in the framework of the Perdew-Burke-Ernzerhof type generalized gradient approximation of the density functional theory. Wang et al [14] calculated the electronic structures of  $Sb_2T_3$  and  $Bi_2Te_3$

crystals using the first-principles full potential linearized augmented plane-wave method. Yavorsky et al [15] performed calculations of the electronic structures of  $Sb_2T_3$  and  $Bi_2Te_3$  compounds by means of the screened Korringa-Kohn-Rostoker (KKR) Green's function method in the atomic sphere approximation (ASA) within local density approximation of the density functional theory.

As far as we know, no *ab initio* general potential calculations of the density of state and charge and the optical properties of the  $Sb_2Te_3$  and  $Bi_2Te_3$  have been reported in detail. In the present work, we have investigated the structural, electronic, and photon energy-dependent optical properties of the  $Sb_2S_3$  and  $Sb_2Se_3$  crystals. The method of calculation is given in Section 2; the results are discussed in Section 3. Finally, the summary and conclusion are given in Section 4.

## II. METHOD OF CALCULATION

Our calculations have been performed using the density functional formalism and local density approximation (LDA) [16] through the Ceperley and Alder functional [17] as parameterized by Perdew and Zunger [18] for the exchange-correlation energy in the SIESTA code [19, 20]. This code calculates the total energies and atomic forces using a linear combination of atomic orbitals as the basis set. The basis set is based on the finite range pseudoatomic orbitals (PAOs) of the Sankey-Niklewsky type [21], generalized to include multiple-zeta decays.

The interactions between electrons and core ions are simulated with separable Troullier-Martins [22] norm-conserving pseudopotentials. We have generated atomic pseudopotentials separately for atoms, Sb, Bi and Te by using the  $5s^25p^3$ ,  $6s^26p^3$  and  $5s^25p^4$  configurations, respectively. The cut-off radii for present atomic pseudopotentials are taken as s: 3.82 au, p: 1.71 au, 2.92 au for the d and f channels of Bi, s:3.62 au, p:2.40 au, 2.78 au for the d and f channels of Te and 2.35 for the s, p, d and f channels of Sb.

Siesta calculates the self-consistent potential on a grid in real space. The fineness of this grid is determined in terms of an energy cut-off  $E_c$  in analogy to the energy cut-off when the basis set involves plane waves. Here by using a double-zeta plus polarization (DZP) orbitals basis and the cut-off energies between 100 and 500  $Ry$  with various basis sets, we found an optimal value of around 425  $Ry$  for  $Sb_2Te_3$  and  $Bi_2Te_3$ . For the final computations, 54 k-points for  $Sb_2Te_3$  and

$\text{Bi}_2\text{Te}_3$  were enough to obtain the converged total energies  $\Delta E$  to about 1meV/atoms.

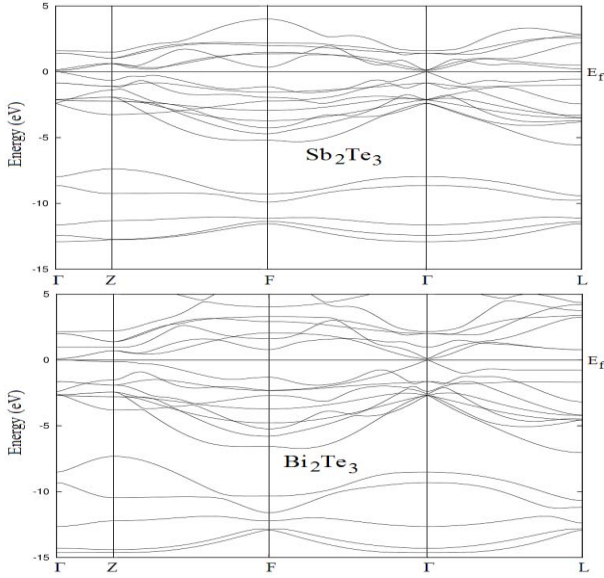


Figure 1. Energy band structure for  $\text{Sb}_2\text{Te}_3$  and  $\text{Bi}_2\text{Te}_3$ .

### III. RESULTS AND DISCUSSION

#### A. Structural properties

- Density of States and Band Structure

All physical properties are related to the total energy. For instance, the equilibrium lattice constant of a crystal is the lattice constant that minimizes the total energy. If the total energy is calculated, any physical property related to the total energy can be determined.

For  $\text{Sb}_2\text{Te}_3$  and  $\text{Bi}_2\text{Te}_3$ , structures which are rhombohedral are considered. The equilibrium lattice parameters, the bulk modulus, and its pressure derivative have been computed minimizing the crystal's total energy calculated for the different values of lattice constant by means of Murnaghan's equation of states (eos) [23]. The lattice constants for  $\text{Sb}_2\text{Te}_3$  and  $\text{Bi}_2\text{Te}_3$  compounds are found to be  $a = 4.256 \text{ \AA}$ ,  $b = 30.397 \text{ \AA}$  and  $a = 4.383 \text{ \AA}$ ,  $b = 30.487 \text{ \AA}$ , respectively. The lattice parameters obtained are in a good agreement with the experimental and theoretical values [24, 14]. In all our calculations, we have used the computed lattice constants. In the present case, the calculated bulk moduli for  $\text{Sb}_2\text{Te}_3$  and  $\text{Bi}_2\text{Te}_3$  are 80.01 and 59.02 GPa, respectively. Unfortunately, there are no theoretical and experimental results for comparing with calculated bulk modulus.

- Charge Density

The three-dimensional valance charge density distribution of  $\text{Sb}_2\text{Te}_3$  and  $\text{Bi}_2\text{Te}_3$  compounds in the plane containing Sb-Te and Bi-Te bonds is illustrated in Fig. 3 and Fig. 4. Examination of the nature of chemical bonding, especially the distribution of valance charges between atoms is necessary to explain the overall shape. The overall shape of the charge distributions suggests covalent bonding of Sb-Te and Bi-Te.

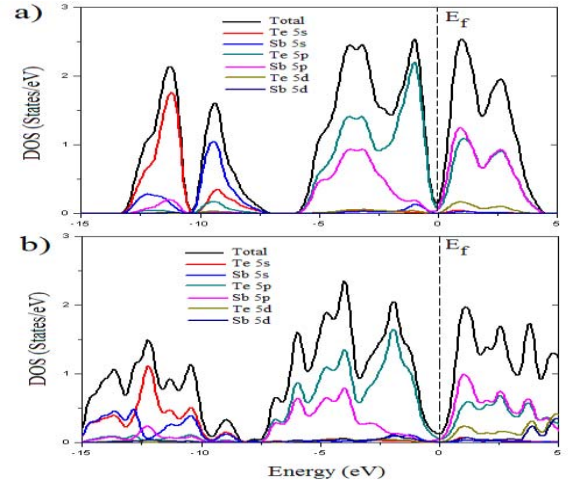


Figure 2. The total (DOS) and projected density of states for a)  $\text{Sb}_2\text{Te}_3$  and b)  $\text{Bi}_2\text{Te}_3$ .

Ionicity is directly associated with the character of the chemical bond. It provides us a mean for explaining and classifying the properties of V-VI compounds. The ionicity character is dependent on the total valance charge density by calculating the charge distribution. We have used an empirical formula [25] to obtain an estimated value of the ionicity factor for  $\text{Sb}_2\text{Te}_3$  and  $\text{Bi}_2\text{Te}_3$  compounds. In this approach the ionicity parameter is defined as

$$f_i = \frac{1}{2} \left( 1 - \cos \left( \frac{E_{AS}}{E_{VB}} \right) \right)$$

Where  $E_{AS}$  is the anti-symmetry gap between the two lowest valance bands and the  $E_{VB}$  the total valance band width. The calculated value of the ionicity factor for  $\text{Sb}_2\text{Te}_3$  is 0.089 for  $E_{AS} = 1.173 \text{ eV}$  and  $E_{VB} = 13.192 \text{ eV}$ , whereas The calculated value of the ionicity factor for  $\text{Bi}_2\text{Te}_3$  is 0.089 for  $E_{AS} = 0.631 \text{ eV}$  and  $E_{VB} = 14.643 \text{ eV}$ .

#### B. Electronic Properties

The energy band structures calculated using LDA for  $\text{Sb}_2\text{Te}_3$  and  $\text{Bi}_2\text{Te}_3$  are shown in Fig. 1. As can be seen in Fig. 1, the  $\text{Sb}_2\text{Te}_3$  and  $\text{Bi}_2\text{Te}_3$  compounds have a direct band gap semiconductor with the value  $0.093 \text{ eV}$  and  $0.099 \text{ eV}$ , respectively. The top of the valance band and the bottom of the conduction band for both compounds positioned at the  $\Gamma$  point of BZ. In conclusion, our band gap values obtained are

in good agreement with theoretical values and the band gaps have same character with given in Ref. [6, 7]. Band structures of  $\text{Sb}_2\text{Te}_3$  and  $\text{Bi}_2\text{Te}_3$  single crystals are compared, band structures of these crystals are highly resemble one another. Thus, on formation of the band structures of  $\text{Sb}_2\text{Te}_3$  and  $\text{Bi}_2\text{Te}_3$  the 5s 5p orbitals of Te atoms are more dominant than 5s5p and 6s6p orbitals of Sb and Bi atoms.

The total and partial densities of states of  $\text{Sb}_2\text{Te}_3$  and  $\text{Bi}_2\text{Te}_3$  are illustrated in Fig. 2. As you can see, from this figure, the lowest valance bands occur between about -14 and -12 eV are dominated by Sb 5s and Bi 6s states while valence

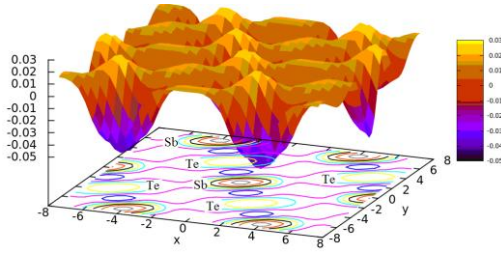


Figure 3. Charge density distribution of the valence charge of  $\text{Sb}_2\text{Te}_3$

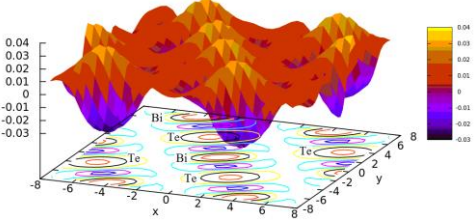


Figure 4. Charge density distribution of the valence charge of  $\text{Bi}_2\text{Te}_3$

bands occur between about  $-12$  and  $-10$  eV are dominated by Te 5s states. The highest occupied valence bands are essentially dominated by Te 5p states. The 5p (6p) states of Sb (Bi) atoms are also contributing to the valence bands, but the values of densities of these states are so small compared to Te 5p states. The lowest unoccupied conduction bands just above Fermi energy level are dominated by Sb 5p and Bi 6p states. The 5p states of Te atoms are also contributing to the conduction bands, but the values of densities of these states are so small compared to Sb 5p and Bi 6p states.

### C. Optical Properties

The  $\text{Sb}_2\text{Te}_3$  and  $\text{Bi}_2\text{Te}_3$  single crystals have an rhombohedral structure that is optically a uniaxial system. For this reason, the linear dielectric tensor of the  $\text{Sb}_2\text{Te}_3$  and  $\text{Bi}_2\text{Te}_3$  compounds have two independent components that are the diagonal elements of the linear dielectric tensor. We first calculated the real and imaginary parts of the x- component of the frequency-dependent linear dielectric function and these are shown in Fig. 5. The  $\epsilon_1^x$  behaves mainly as a classical oscillator. It vanishes (from positive to negative) at about  $1.27$  eV,  $6.98$  eV,  $10.24$  eV and  $17.32$  eV (see Fig. 5) for  $\text{Sb}_2\text{Te}_3$  compound. The  $\epsilon_1^x$  is equal to zero at about  $1.89$  eV,  $6.55$  eV,  $7.63$  eV and  $17.41$  eV (see Fig. 5) for  $\text{Bi}_2\text{Te}_3$  compound. The peaks of the  $\epsilon_2^x$  correspond to the optical transitions from the valence band to the conduction band and are in agreement with the previous results. The maximum peak value of  $\epsilon_2^x$  for  $\text{Sb}_2\text{Te}_3$  are around  $1.24$  eV, whereas the maximum value of  $\epsilon_2^x$  for  $\text{Bi}_2\text{Te}_3$  are around  $1.74$  eV. Spectral dependences of dielectric functions show the similar features for both materials because the electronic configurations of Sb ( $[\text{Kr}], 3d^{10} 4s^2 4p^6$ ) and Bi ( $[\text{Xe}], 4d^{10} 5s^2 5p^6$ ) are very close to each other. In general, there are various contributions to the dielectric function, but Fig. 5 show only the contribution of the electronic polarizability to the dielectric function. In the range between  $0.2$  eV and  $3$  eV,  $\epsilon_1^x$

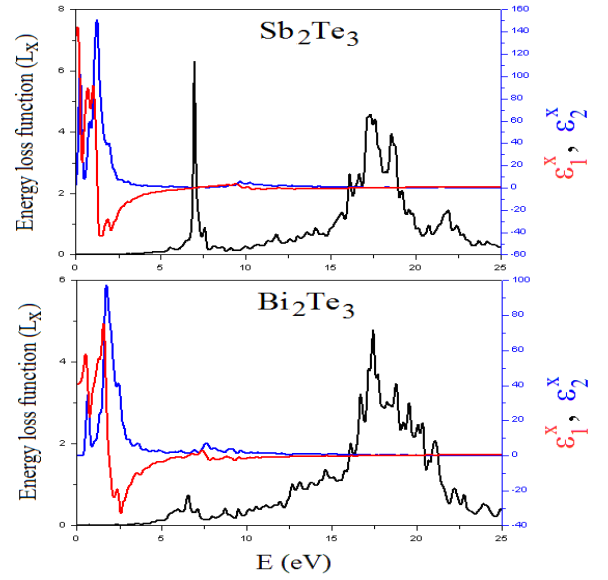


Figure 5. Energy spectra of dielectric function and energy-loss function ( $L$ ) along the x for  $\text{Sb}_2\text{Te}_3$  and  $\text{Bi}_2\text{Te}_3$ .

decrease with increasing photon-energy, which is characteristics of an anomalous dispersion. In this energy range, the transitions between occupied and unoccupied states mainly occur between Te 5p states which can be seen in the DOS displayed in Fig. 2. Furthermore as can be seen from Fig. 5, the photon-energy range up to  $0.1$  eV is characterized by high transparency, no absorption and a small reflectivity. The  $0.1$ - $3.0$  eV photon energy range is characterized by strong absorption and appreciable reflectivity. The absorption band extending beyond  $7$  eV up to  $10$  eV is associated with the transitions from the low-lying valence subband to conduction band. Second, we see that above  $8$  eV, corresponding to the Sb 5s (Bi 6s) and Te 5p. Also, we remark that the region above  $10$  eV cannot be interpreted in term of classical oscillators. Above  $10$  eV  $\epsilon_1$  and  $\epsilon_2$  are dominated by linear features, increasing for  $\epsilon_1$  and decreasing for  $\epsilon_2$ .

The corresponding energy-loss functions,  $L(\omega)$ , are also presented in Fig. 5. In this figure,  $L_x$  correspond to the energy-loss function along the x- direction. The function  $L(\omega)$  describes the energy loss of fast electrons traversing the material. The sharp maxima in the energy-loss function are associated with the existence of plasma oscillations [26]. The curves of  $L_x$  for  $\text{Sb}_2\text{Te}_3$  and  $\text{Bi}_2\text{Te}_3$  in Fig. 5 have a maximum near  $17.32$  and  $17.42$  eV, respectively.

Also, we calculated effective number of valence electrons  $N_{eff}$  and the effective dielectric constant  $\epsilon_{eff}$ . The effective optical dielectric constant,  $\epsilon_{eff}$  reaches a saturation value at about  $9$  eV. The photon-energy dependence of  $\epsilon_{eff}$  can be separated into two regions. The first is characterized by a rapid rise and it extends up to  $4$  eV. In the second region the value of  $\epsilon_{eff}$  rises more smoothly and slowly and tends to saturations at the energy  $9$  eV. This means that the greatest

contribution to  $\varepsilon_{eff}$  arises from interband transitions between 0 eV and 4 eV .

As states above, the  $N_{eff}$  is the effective number of valance electrons per unit cell at the energy  $\hbar\omega_0$  (under the condition that all the interband transitions possible at this frequency  $\omega_0$  were made). In the case of  $Sb_2Te_3$  and  $Bi_2Te_3$  the value of  $N_{eff}$  increases with increasing photon energy and has tendency to saturate near 9 eV and 20 eV . Therefore, each of our plots of  $N_{eff}$  versus the photon energy for  $Sb_2Te_3$  and  $Bi_2Te_3$  can be arbitrarily divided into two part. The first is characterized by a rapid growth of  $N_{eff}$  up to  $\sim 5$  eV and extend to 10 eV . The second part shows a smoother and slower growth of  $N_{eff}$  and tends to saturate at energies above 30 eV . It is therefore so difficult to choose independent criteria for the estimate of the of valance electrons per unit cell. Recognizing that the two valance subbands are separated from each other and are also separated from the low-lying states of the valance band, we can assume a tendency to saturation at energies such that the transition from the corresponding subbands are exhausted. In other words, since  $N_{eff}$  is determined only by the behavior of  $\varepsilon_2$  and is the total oscillator strengths, the sections of the  $N_{eff}$  curves with the maximum slope, which correspond to the maxima  $dN_{eff} / d\hbar\omega$ , can be used to discern the appearance of new absorption mechanism with increasing energy (E=3.8 eV , 9.5 eV for  $Sb_2Te_3$  and E=4.2 eV , 9 eV for  $Bi_2Te_3$ ). The values and behavior of  $N_{eff}$  and  $\varepsilon_{eff}$  very close to each other.

#### IV. CONCLUSION

In present work, we have made a detailed investigation of the structural, electronic, and frequency-dependent linear optical properties of the  $Sb_2Te_3$  and  $Bi_2Te_3$  crystals using the density functional methods. The results of the structural optimization implemented using the LDA are in good agreement with the experimental and theoretical results. We have examined photon-energy dependent dielectric functions, some optical properties such as the energy-loss function, the effective number of valance electrons and the effective optical dielectric constant along the x- axis.

#### REFERENCES

- [1] C. L. Kane, and E. J. Mele, "Z<sub>2</sub> topological order and the quantum spin hall effect", Phys. Rev. Lett. vol. 95, pp. 146802.1-146802.4, September 2005.
- [2] B. A. Bernevig, and S. C. Zhang, "Quantum spin hall effect", Phys. Rev. Lett. vol 96, pp. 106802.1-106802.4, March 2006.
- [3] J. E. Moore, and L. Balents, "Topological invariants of time-reversal-invariant band structures", Phys. Rev. B, vol. 75, pp. 121306.1-121306.4, March 2007.
- [4] F. Liang, C. L. Kane, and E. J. Mele, "Topological insulators in three dimensions", Phys. Rev. Lett., vol. 98, pp. 106803.1-106803.4, March 2007.
- [5] F. Liang, C. L. Kane, "Topological insulators with inversion symmetry", Phys. Rev. B , vol. 76, pp. 045302.1-0.45302.17, July 2007.
- [6] W. Zhang, R. Yu, H. -J. Zhang, X. Dai, and Z. Fang, "First-principles studies of the three-dimensional strong topological insulator  $Bi_2Te_3$ ,  $Bi_2Se_3$  and  $Sb_2Te_3$ ", New J. Phys., vol. 12, pp. 065013.1-165013.14, June 2010.
- [7] H. Zhang, C. -H. Liu, X. -L. Qi, X. Dai, Z. Fang, and S.-C. Zhang, "Topological insulators in  $Bi_2Te_3$ ,  $Bi_2Se_3$  and  $Sb_2Te_3$  with a single Dirac cone on the surface", Nature Physics, vol. 5, pp. 438-442, May 2009..
- [8] L. G. Khvostantsev, A. I. Orlov, N. K. Abrikosov, T. E. Svechnikova, and S. N. Chizhevskaya, "Thermoelectric properties and phase transitions in  $Bi_2Te_3$  under hydrostatic pressure up to 9 GPa and temperature up to 300 C°", Phys. Stat. Sol. (a), vol. 71, pp. 49-53,(1982) 49-53, May 1982.
- [9] J. I. Zhang, S. J. Zhang, H. M. Weng, W. Zhang, L. X. Yang, Q. Q. Liu, S. M. Feng, X. C. Wang, R. C. Yu, L. Z. Cao, L. Wang, W. G. Yang, H. Z. Liu, W. Y. Zhao, S. C. Zhang, X. Dai, Z. Fang, and C. Q. Jin, "Pressure-induced superconductivity in topological parent compound  $Bi_2Te_3$ ", Proc. Nat. Acad. Sci., vol. 108, pp. 24-28, January 2011.
- [10] D. D. Frari, S. Diliberto, N. Stein, and J. M. Lecuire, "Comparative study of the electrochemical preparation of  $Bi_2Te_3$ ,  $Sb_2Te_3$  and  $(Bi_xSb_{1-x})_2Te_3$ ", Thin Solid Films, vol. 483, pp. 44-49, February 2005.
- [11] B. C. Sales, "Thermoelectric materials", Science, vol. 295, pp. 1248-1249, February 2002.
- [12] M. J. Huang, R. H. Yen, and A. B. Wang, "The influence of the Thomson effect on the performance of a thermoelectric cooler", Int. J. Heat Mass Transfer, vol. 48, pp. 413-418, January 2005.
- [13] P. P. Dradyumnan, P. P. Swathikrishnan, "Thermoelectric properties of  $Bi_2Te_3$  and  $Sb_2Te_3$  and its bilayer thin films", Indian J. Pure and Appl. Phys., vol. 48, pp. 115-120, February 2010.
- [14] G. Wang, and T. Cagin, "Electronic structure of the thermoelectric materials  $Bi_2Te_3$  and  $Sb_2Te_3$  from first-principles calculations", Phys. Rev. B , vol. 76, pp. 075201.1-075201.8, August 2007.
- [15] B. Y. Yavorsky, N. F. Hinsche, I. Mertig, and P. Zahn, "Electronic structure and transport anisotropy of  $Bi_2Te_3$  and  $Sb_2Te_3$ ", Phys. Rev. B, vol. 84, pp. 165208.1-165208.7, October 2011.
- [16] J. W. Kohn, and L. J. Sham, "Self-consistent equations including exchange and correlation effects", Phys. Rev., vol. 140, pp. A1133-A1138, November 1965.
- [17] D. M. Ceperley, and M. J. Adler, "Ground state of the electron gas by a stochastic method", Phys. Rev. Lett., vol. 45, pp. 566-569, August 1980.
- [18] P. Perdew, and A. Zunger, "Self-interaction correction to density-functional approximations for many-electron systems", Phys. Rev. B, vol. 23, pp. 548-5079, May 1981.
- [19] P. Ordejón, E. Artacho, and J. M. Soler, "Self-consistent order-N density-functional calculations for very large systems", Phys. Rev. B, vol. 53, pp. R10441-R10444, April 1996.
- [20] J. M. Soler, E. Artacho, J. D. Gale, A. Garcia, J. Junquera, P. Ordejón, and D. Sánchez-Portal, "The SIESTA method for ab initio order-N materials simulation", J. Phys. Condens. Matt., vol. 14, pp. 2745-2779, Mart 2002.
- [21] O.F. Sankey, and D.J. Niklewski, "Ab initio multicenter tight-binding model for molecular dynamics simulations and other applications in covalent systems", Phys. Rev. B, vol. 40, pp. 3979-3995, 1989.
- [22] N. Troullier, and J. L. Martins, " Efficient pseudopotentials for plane-wave calculations", Phys. Rev. B, vol. 43, pp. 1993-2006, January 1991.
- [23] F. D. Mumaghan, "The compressibility of media under extreme pressures", Proc Natl. Acad. Sci. U.S.A., vol. 50, pp. 244-247, September 1944.
- [24] R. W. G. Wyckoff, Crystal Structures, Wiley, New York, vol. 2, 1964, pp.30.
- [25] L. Marton, "Experiments on low-energy electron scattering and energy loss", Rev. Mod. Phys.,vol. 28, pp. 172-183, July 1956.
- [26] K. Unger, and H. Newman, "The antisymmetric gap and the total width of the valance band of binary compound crystals ", Phys. Status Solidi B, vol. 64, pp. 117-122, July 1974